Statistical Properties of Low-Frequency Magnetic Field Fluctuations in the Solar Wind From 0.29 to 1.0 AU During Solar Minimum Conditions: HELIOS 1 and HELIOS 2

K. U. Denskat and F. M. Neubauer

Institut für Geophysik und Meteorologie der Technischen Universität Braunschweig, D-3300 Braunschweig, Federal Republic of Germany

To obtain information on the temporal and spatial evolution of MHD waves and discontinuities in the solar wind, we studied by means of statistical methods magnetic field fluctuations measured by the two HELIOS spacecraft in the frequency range between 2.4×10^{-5} Hz and 1.3×10^{-2} Hz at distances from the sun between 0.29 AU and 1.0 AU. Some statistical properties as magnetic field variances show the fluctuations remaining very similar on their way out from the sun. A different picture of the fluctuations emerges from analyzing the spectral properties of the magnetic field: The slope of the power spectral densities (both the vector components and the magnitude of the magnetic field) as a function of frequency becomes steeper with increasing heliographic distance—the solar wind seems to act as a low-pass filter. The major changes occur within a heliographic distance up to about 0.4 AU. Field magnitude fluctuations fall off less rapidly with increasing radius than do fluctuations in the vector components. Cross spectral analysis between magnetic field components reveal the fluctuations as generally being field magnitude conserving.

1. Introduction

Starting with *Coleman* [1966], *Belcher et al.* [1969], and *Belcher and Davis* [1971], numerous observations of low-frequency MHD fluctuations in the solar wind plasma and magnetic field have been reported. The correlation between magnetic field and solar wind velocity fluctuations has been taken as evidence for the fluctuations to be Alfvénic. This term was introduced by *Belcher and Davis* [1971] because these disturbances have some characteristics in common with linear Alfvén waves, although their amplitude is usually not small. Besides Alfvénic fluctuations the existence of discontinuities and the rare occurence of other wave modes has been shown [*Burlaga,* 1971]. A recent review on the theory and observations of hydromagnetic waves and turbulence in the solar wind is available from *Barnes* [1979], and a review with special emphasis on Alfvénic fluctuations in the inner solar system is available from *Burlaga* [1979]. An alternative to interpreting the solar wind fluctuations in terms of waves is to consider the solar wind as a turbulent medium. *Coleman* [1968] interpreted power spectra of the magnetic field and the radial component of the solar wind velocity in terms of turbulence by using *Kraichnan*'s [1965] incompressible MHD turbulence theory. *Dobrowolny et al.* [1980a, b] suggest that a turbulent description can easily account for the properties indicated by present observations and is more appropriate than a description in terms of simple waves. This MHD turbulence would be characterized, to a good degree, by the absence of nonlinear wave interactions and would necessarily be a mixture of modes with polarization of Alfvénic and slow magnetosonic types. The apparent contradiction—the absence of nonlinear wave interactions and the presence of an almost structureless power spectrum—is explained in their work by the interpretation that the absence of nonlinear wave interactions is a general consequence of the relaxation of an initial MHD turbulence

field, provided that this initial turbulence is asymmetric, i.e., favors one sense of propagation of the Alfvénic fluctuations parallel or antiparallel to the mean field. In this paper we shall discuss the statistical results obtained from HELIOS observations from the viewpoints of both turbulence and waves.

Both HELIOS spacecraft provide continuous plasma and magnetic field data at distances from the sun from 1.0 AU down to 0.29 AU. With these data there exists the unique opportunity to analyze plasma and magnetic field fluctuations over several solar rotations at quite different distances from the sun. Besides the possible influences of time variations and a heliographic latitude dependence, we are able to study the evolution of these fluctuations on their way from 0.29 AU to 1.0 AU.

The time intervals chosen for investigation were such as to provide maximum data coverage under 'stable' interplanetary conditions. This requirement was fulfilled during about the first 110 days after the launch of HELIOS 1 in December 1974 and of HELIOS 2 in January 1976. These time intervals fell into the period of declining and minimum solar activity, where the interplanetary stream structure was simple and characterized by stable recurrent high speed streams [*Rosenbauer et al.,* 1977; *Marsch et al.,* 1982].

The plan of the paper is the following: section 2 gives a survey on the experiment and the data. In section 3 general statistical properties of the fluctuations are studied by computing magnetic field variances at different heliographic distances. Section 4 contains the method and the results from power spectral analysis. Examples of magnetic field power spectral densities are given as well as overall statistical properties of the magnetic field power spectra as a function of heliographic distance. After giving some information on the general type of solar wind magnetic field fluctuations in section 5, we summarize our observations in section 6.

2. The Present Analysis

This analysis uses flux gate magnetometer data from the HELIOS 1 and HELIOS 2 spacecraft, which have provided

HELIOS 1   HELIOS 2
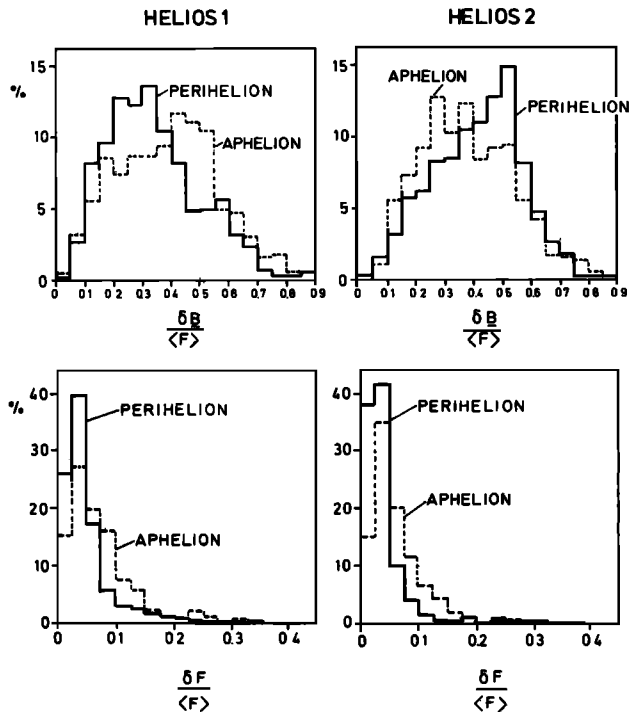
Fig. 1. Distributions of normalized standard deviations of vector magnetic field fluctuations δB and magnetic field magnitude fluctuations δF for 1-hour time intervals normalized by the average field magnitude. The time periods for the calculation cover one solar rotation as seen from the spacecraft for the first aphelion and first perihelion time period of HELIOS 1 and HELIOS 2, respectively. The aphelion period covers a distance range from 0.90 to 0.98 AU, and the perihelion period covers a distance range from 0.31 (HELIOS 1) and 0.29 (HELIOS 2) to 0.50 AU.

solar wind plasma and magnetic field data at heliographic distances between 0.29 AU and 1.0 AU. The Technical University of Braunschweig magnetometer is a three component flux gate magnetometer (Förstersonde) with four automatically switchable measurement ranges of ±100 nT and ±400 nT. The highest resolution is ±0.2 nT, with a maximum sampling rate of 8 vectors/s. Included in the experiment is a mechanical flipper device that makes it possible to flip by command the sensor parallel to the spin axis into the spinning plane of the spacecraft to help determine the zero offset of the Z component parallel to the spin axis. In addition, the offset of the Z component is determined continuously by a correlation technique [Hedgecock, 1975a]. The overall offsets of the components in the spin plane composed of sensor offsets and spacecraft field are removed by properly averaging over the spin variations. A detailed description of the experiment is given by Musmann et al. [1975]

In this study we use 40-s averages of the interplanetary vector magnetic field calculated from samples every 0.25 s most of the time. The time periods analyzed are December 10, 1974, to April 5, 1975 (HELIOS 1), and January 15 to May 5, 1976 (HELIOS 2). These time periods were such as to provide maximum interplanetary data coverage between 0.29 AU and 1.0 AU. To get improved statistical confidence, the analysis of data during other time periods would be desirable. However, the successive continuous calculation of power spectra requires complete data coverage. This demand cannot be fulfilled by other time periods than the ones given above.

Time periods with data including sector boundaries and shock waves have been excluded from the analysis. Only fluctuations with scale lengths up to approximately 0.2 AU have been analyzed. This measure will guarantee influences of different streaming states of the solar wind on the analysis being negligibly small at least in central parts and trailing edges of high speed streams.

For studying MHD fluctuations the components transverse and parallel to the mean field direction are of particular interest. Therefore, we choose the 'mean field' (MF) coordinate system defined such that the Z axis is taken along the average direction of the vector magnetic field (over the time period of the analysis), the X axis is perpendicular to Z and lies in the XZ_{SE} plane (XZ of the solar ecliptic coordinate system) and Y completes the right-handed orthogonal set.

Thus the unit vectors of this reference frame are given by

$$\hat{X} = \frac{\langle \mathbf{B} \rangle \times \mathbf{r}_{XZ}}{|\langle \mathbf{B} \rangle \times \mathbf{r}_{XZ}|}$$

$$\hat{Y} = \frac{\langle \mathbf{B} \rangle \times (\langle \mathbf{B} \rangle \times \mathbf{r}_{XZ})}{|\langle \mathbf{B} \rangle \times (\langle \mathbf{B} \rangle \times \mathbf{r}_{XZ})|}$$

$$\hat{Z} = \frac{\langle \mathbf{B} \rangle}{|\langle \mathbf{B} \rangle|}$$

where $\mathbf{r}_{XZ} = \langle B_{X_{SE}} \rangle \hat{\imath} + \langle B_{Z_{SE}} \rangle \hat{k}$ with the unit vectors $\hat{\imath}$ and $\hat{k}$ in the X_{SE} and Z_{SE} direction, respectively.

3. THE DISTRIBUTION OF MAGNETIC FIELD VARIANCES

To determine the general fluctuation properties at different heliographic distances, we calculated for one hour intervals the root mean square (rms) or standard deviations δF and δB, where δF is the rms deviation of field magnitude fluctuations, and δB is the rms deviation of vector field fluctuations with contributions from both magnitude and directional variations. The rms deviation δB is computed from the individual rms deviations according to $\delta B = (\delta B_X{}^2 + \delta B_y{}^2 + \delta B_Z{}^2)^{1/2}$. This was done with the data of the first 110 days of each HELIOS mission. With increasing magnetic field magnitude F the standard deviations of the components and field magnitude are increasing as well. The magnitude F shows a distance dependence proportional to $r^{-1.6}$ in the case of HELIOS 1 [Musmann et al., 1977]. In order to get proper criteria for comparison of the fluctuations at different heliographic distances, we normalize the standard deviations given above by the corresponding one hour averages of the magnetic field magnitude. Figure 1 shows the normalized standard deviations for the vector field fluctuations and for the field magnitude fluctuations for both spacecraft under perihelion and aphelion magnetic field conditions. Apparently, there are no significant differences in the class of directional fluctuations. However, the distributions of $\delta F/\langle F \rangle$ are broader for the aphelion periods than for the perihelion periods, possibly indicating a different composition of MHD waves and discontinuities at different distances from the sun.

Earlier studies of the radial dependence of specifically Alfvénic fluctuations seen in Mariners 4 and 5 magnetic and plasma data over the distance range between 0.7 and 1.6 AU [Belcher and Burchsted, 1974] and of transverse fluctuations seen in the magnetic field data from Pioneer 10 for distances out to 3.3 AU [Rosenberg et al., 1978] were consistent with

the presence of a field of Alfvénic turbulence being convected by the solar wind with little or no local generation or dissipation of waves.

4. THE POWER SPECTRAL ANALYSIS

4.1. The Method

For the computation of power spectra and cross spectra between magnetic field components and magnitude we generally follow the procedure described by *Bendat and Piersol* [1971, p. 322ff]. The data intervals were chosen such that the number of data points fits a power of 2. This is necessary since we are using the fast Fourier transform technique. The magnetic field averages of 40-s limit the longest wave period that can be analyzed to 11 hours 23 min (by taking 1024 data points for each Fourier transform). Periods up to half a day prove to be a suitable choice in analyzing waves and discontinuities in the solar wind plasma, since longer wave periods will be influenced by the solar wind streaming structure. Of course, even this time period will be too long if waves in leading edges of high speed streams are studied. To avoid remaining influences of the solar wind streaming structure (and waves with periods longer than the data interval analysed) low order trends were removed by subtracting the values predicted by a 'least squares' fitted second order polynomial. After the data were reduced to zero mean and data gaps were filled by zeros the data sequence was tapered by a cosine taper data window. Then the Fourier transform was performed and the raw spectral estimates were computed. The raw spectral estimates were frequency averaged to obtain the desired degree of freedom, which is 32 in our analysis. The corresponding normalized standard error is then 0.25.

We tested the algorithm extensively. A helpful tool was proposed by *Owens* [1978]. Given an arbitrary power spectrum, one can generate the corresponding fluctuations in the time domain. In this way it is possible to check, e.g., the influence of data gaps on the power spectral density and cross-spectra by including data gaps of different size into the generated time series, computing the corresponding spectrum and comparing it with the originally given one. Further, the algorithm allows a definitive prediction if prewhitening is necessary for the expected power spectral densities. The latter turned out not to be a worthwhile procedure for conditions generally found in solar wind magnetic field fluctuations. Data gaps are a general serious problem in computing power spectral densities, especially if the gaps are regular in occurrence. We limited our analysis to data sequences having data gaps less than 5%. We further excluded a data sequence from the analysis, if the data breaks appeared to be regular in occurrence. Since missing data are filled by zeros (zero being the most probable value in the Gaussian amplitude distribution of prepared data) jumps at the beginning and end of data gaps may cause power enhancements that are quite difficult to estimate. However, a contribution to the total power density owing to data gaps may be computed from applying Parseval's Theorem (e.g., *Jenkins and Watts* [1968], p. 215). This approach was also used successfully by *Hedgecock* [1975b], who checked and corrected amplitudes of magnetic field power spectral densities by fulfilling this condition. We only accepted power spectral densities and cross spectra for further analysis if

Parseval's theorem

$$\sigma^2 = \int_{f_1}^{f_2} P(f)df$$

and

$$c^2 = \int_{f_1}^{f_2} L(f)df$$

(*Jenkins and Watts* [1968], p. 345) were fulfilled, where σ^2 is the variance of the field component or magnitude, $P(f)$ is the power spectral density, c^2 is the cross covariance, $L(f)$ is the cospectrum, and f_1 and f_2 are the frequency limits of the spectrum. The equations were considered to be fulfilled if the two sides of the equations did not differ by more than 0.1%.

The noise sources—quantization and instrument noise—are both below 10^{-1} nT²/Hz at the highest frequency inherent in the analysis. Under solar wind magnetic field conditions during the time intervals of investigation the power spectral densities generally exceeded 10^{-1} nT²/Hz in the frequency band from 2.4×10^{-5} Hz to 1.3×10^{-2} Hz (see also Figure 3).

4.2. Power Spectral Densities from 11 1/2 Hours Data Sequences

We computed continuous power spectra from 11 1/2 hour data sequences overlapping by half an hour over the first 110 (115) days of each HELIOS mission for the three vector components (MF coordinates) and the magnitude of the magnetic field. Owing to a large number of data gaps, only a small number of spectra (75) could be computed from the HELIOS 1 data. Therefore, we restrict the statistical results of spectral analysis shown to HELIOS 2 giving us a number of 161 spectra during this time period.

Two examples of power spectra are shown at different distances from the sun (Figure 2). These power spectra are quite representative for the locality where the data have been taken. The power spectral density increases as the sun is approached. In addition, the slope of the power spectral density as a function of frequency changes significantly. The spectra are flatter at 0.29 AU than at 0.97 AU, where the major differences seem to occur at low frequencies below, say, 2×10^{-3} Hz. Assuming a power law dependence of the spectral density proportional to $f^{-\alpha}$, the average best fit exponent α (determined by a least squares method) varies between 1.59 and 1.69 (components and magnitude) at 0.97 AU and between 0.87 and 1.15 (components and magnitude) at 0.29 AU. However, at 0.29 AU the power law fit $P \sim f^{-\alpha}$ does not seem to be the best possibility of representing the frequency dependence of the spectral density, since the spectral slope becomes increasingly steeper with increasing frequency. An exponential fit where the power spectral density is proportional to $e^{-\beta f}$ might improve our results. We computed the best fit β for the example shown in Figure 2. We further computed correlation coefficients and variances to be able to compare the two fits. As expected at 0.97 AU, the fit $P \sim f^{-\alpha}$ was quite superior. At 0.29 AU, both fits for the components were almost equally good. For further analysis we used the power law fit $P \sim f^{-\alpha}$ despite the apparent insufficiency at 0.29 AU. Therefore one should keep in mind that the spectral exponent α computed in this way for the whole frequency range from 2.4×10^{-5} Hz to 1.3

HELIOS 2
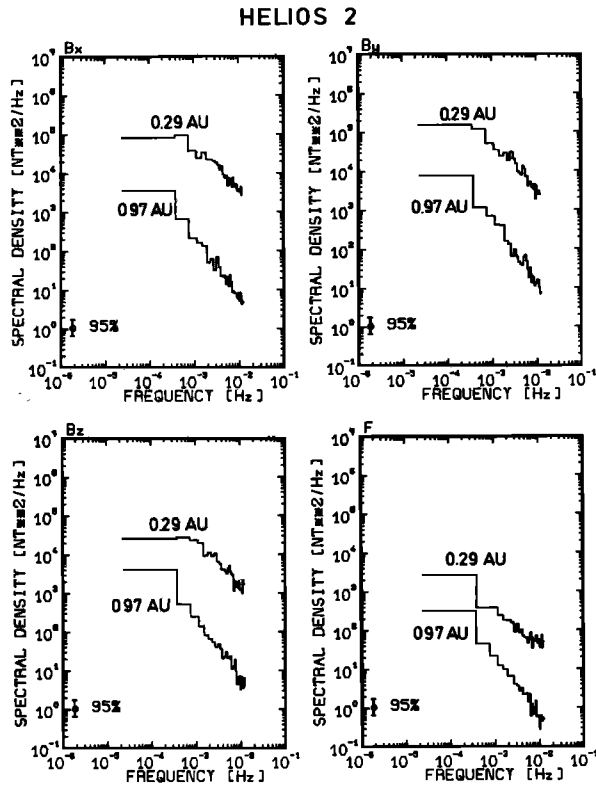
Fig. 2. Magnetic field (vector components and magnitude) power spectral densities at different heliographic distances. The 'mean field' coordinate system (Z axis parallel to the average direction of the vector magnetic field) was used throughout the paper. The spectra were computed from 40-s averages of the magnetic field over 11 1/2 hours on January 24, 1900 UT to January 25, 0623 UT, 1976 (0.97 AU) and on April 14, 2300 UT to April 15, 1023 UT, 1976 (0.29 AU). Also given are the 95% confidence limits for the spectral density computed from an equivalent of 32 degrees of freedom.

$\times$ 10^{-2} Hz may be misleading at least under perihelion conditions, where the spectra are significantly flatter at low frequencies than at high frequencies.

Figures 3, 4, and 5 give general information about the radial dependence of power spectral densities and the steepness of the spectra for 110 days of data. The average total power spectral densities in the magnetic field components P_T (trace of power spectral matrix) of different frequency bands show for all frequencies a general decrease from 0.29 to 1.0 AU (Figure 3). For all frequencies the spectral density changes most rapidly at smaller heliographic distances. At larger heliographic distances from 0.6 to 1.0 AU the decrease in spectral density is less. The decrease in spectral density as a function of heliographic distance is smaller for low frequency than for high frequency fluctuations. The drop in spectral density between 0.55 and 0.60 AU is due to very small wave activity in low speed solar wind plasma.

Figure 4 shows the distributions of the best fit exponent α (assuming the power spectral densities being proportional to $f^{-\alpha}$) for different heliographic distance ranges. The distributions of the best fit exponent for the field components and the field magnitude differ little, whereas the distribution for the magnitude is slightly broader. As the sun is approached the best fit exponent changes from a mean of 1.5 to 1.6 to a mean close to 1. The fluctuations become 'whiter' at smaller heliographic distances. This change does not occur continuously over the distance range of 0.71 AU but rather abruptly
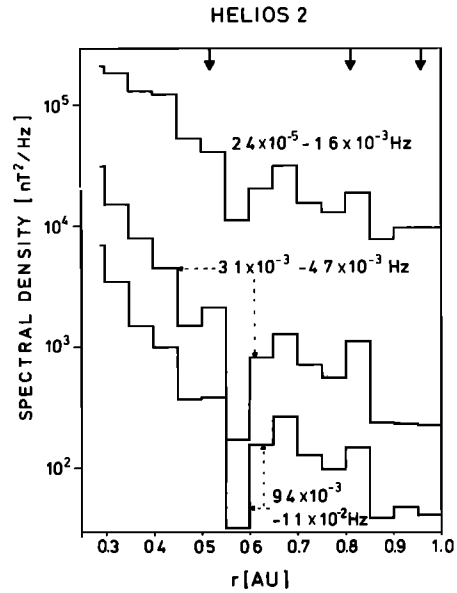
HELIOS 2

Fig. 3. Average total power spectral densities P_T in the magnetic field components (trace of the power spectral matrix) from HELIOS 2 for three different frequency ranges as a function of distance from January 15 to May 5, 1976. A total of 161 spectra was used to compute the average power densities over 0.05 AU distance intervals. Arrows mark the distance range covered during one solar rotation as seen from the spacecraft, respectively. The power densities in the frequency ranges from 1.6 $\times$ 10^{-3} to 3.1 $\times$ 10^{-3} Hz and from 4.7 $\times$ 10^{-3} to 9.4 $\times$ 10^{-3} Hz are omitted for the clearness of the presentation but fit well between the power densities of the frequency ranges shown.

inside 0.40 AU, where the solar wind begins to act as a low-pass filter for MHD fluctuations. The HELIOS 1 spectra based on a smaller number of samples (75) than the HELIOS 2 spectra (161) show the same general behavior. For instance, the mean value of the best fit exponent for the X component changes from 1.36 between 0.31 and 0.40 AU to 1.58 between 0.85 and 1.0 AU.

Average power spectral densities of the magnetic field
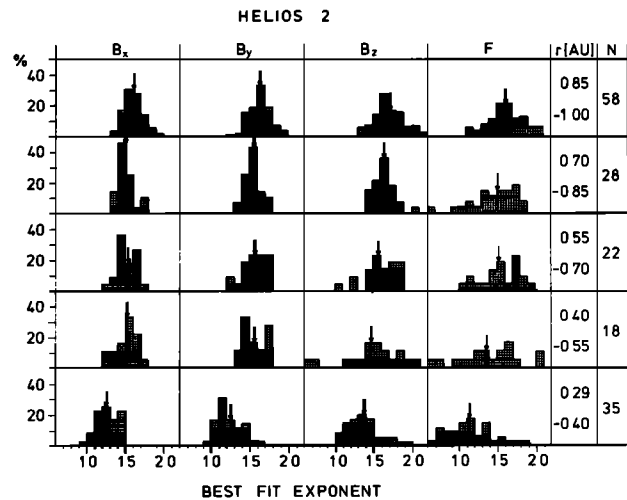
Fig. 4. Distributions of best fit exponents α from HELIOS 2 (assuming the power spectral density being proportional to $f^{-\alpha}$) within 5 different heliographic distance ranges between 0.29 and 1.0 AU for the vector components and the magnitude of the magnetic field. N gives the number of samples in each distance interval. Arrows mark the mean values of the distributions.

magnitude P_F (not shown here) do not reveal such a clear dependence from heliographic radius. There is a general decrease of the power density with increasing radius, but there is also a quite larger variability with distance in power density of the field magnitude than of the field components. The reason is that the power density of the field magnitude in the leading edge of a high speed stream may be two orders of magnitude larger than in the central part or in the trailing edge of the same stream, which is quite different from the observed behavior of field component power densities in different parts of a stream. Neglecting the stream structure dependent high variability of the field magnitude power density, it appears that the field magnitude power density falls off less rapidly with increasing heliographic distance than the field component power density. This indicates a different evolution of compressive fluctuations with increasing distance than of directional fluctuations and is consistent with earlier findings of *Coleman et al.* [1969] in their Mariner 4 study.

The different evolution with increasing distance of compressive magnitude field fluctuations and directional magnetic field fluctuations is more obvious from Figure 5. The ratio P_T/P_F varies with distance and with frequency. At all frequencies there is a general decrease of P_T/P_F with increasing heliographic distance. In each distance interval there is a typical dependence of P_T/P_F from frequency with maximum values between 4×10^{-4} and 5×10^{-3} Hz and minimum values at the lowest and highest frequencies computed. This dependence is similar at all distances, but almost vanishes between 0.85 and 1.0 AU, where P_T/P_F is approximately constant over the frequency range analyzed.

How do the spectra depend on solar wind stream conditions and how do they vary under different stream conditions with heliographic distance? A clear picture emerges for spectra of directional fluctuations in central parts and trailing edges of high speed streams. Under these stream conditions the steepening of the spectra outside 0.4 AU is most obvious. In low-speed solar wind plasma the spectra are somewhat flatter at all solar distances studied. The difference in the spectral exponent is of the order of 0.2 on the average. This value must be considered with some caution, since only a small number of samples (21 for HELIOS 2) was available in low-speed solar wind. The same is true for spectra in leading edges of high speed streams. As in central parts and trailing edges of high speed streams the spectra seem to be flatter on average under perihelion conditions than under aphelion conditions. However, within leading edges of high speed streams, both flatter and steeper spectra than in the central parts and trailing edges of the same streams are observed. There might be a dependence on the structure of high-speed stream leading edges having sharper boundaries near the sun [*Rosenbauer et al.*, 1977].

If one calculates spectral densities normalized by the squares of the average magnetic field strength as expected, a different behavior of normalized spectral densities as a function of radius emerges for different frequency ranges. The normalized spectral densities of vector component low-frequency fluctuations (frequency range from 2.4×10^{-5} to 1.6×10^{-3} Hz) remain relatively constant at heliographic distances from 0.29 to 1.0 AU, while normalized spectra of higher frequencies (frequency range from 1.6×10^{-3} to 1.3×10^{-2} Hz) decrease with increasing radius to 1/4 of the value at 0.29 AU. The normalized spectral densities of field magni-
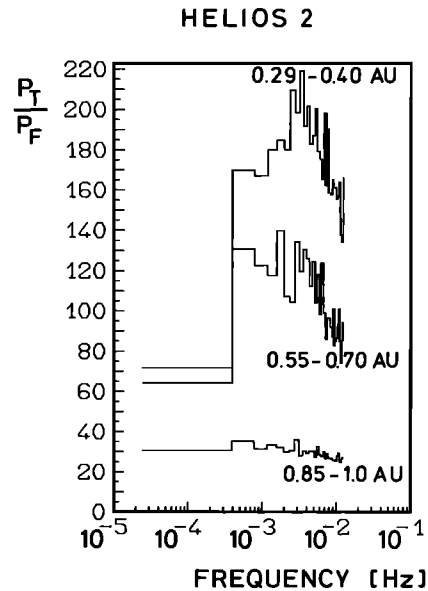
HELIOS 2

Fig. 5. Average ratio P_T/P_F (P_F being the power spectral density in the field magnitude) from HELIOS 2 for three distance ranges as a function of frequency. Number of spectra and time period are the same as in Figure 3. Two distance ranges are omitted for the clearness of the presentation, but the ratio P_T/P_F at these distances is intermediate to the ones shown.

tude fluctuations do not show a decrease with increasing radius, there may even be an increase with increasing radius for all frequencies under investigation.

4.3 Discussion of Observed Power Spectral Densities

Different power spectral densities observed by one spacecraft at different heliographic distances could also be due to different heliographic longitudes and latitudes or a temporal variation. However, there are reasons that let us conclude that the spectral characteristics essentially depend on the distance from the sun besides an additional dependence on stream structure. First, the primary missions of HELIOS 1 and HELIOS 2 were more than one year apart (but under approximately the same solar minimum conditions) and the changes in power spectral densities around 0.40 AU were observed by both spacecraft. Second, in the distance range between 0.29 AU (0.31 AU (HELIOS 1)) and 0.40 AU the two spacecraft observed magnetic field fluctuations during 25 days corresponding to a heliographic longitude range of approximately 200° and a latitude range from −5° to 7.2° (HELIOS 2) and −6.5° to 6.5° (HELIOS 1). In this time period there existed two distinct high speed solar wind streams. The spectral characteristics of magnetic field fluctuations as a function of stream structure changed in the same way as they did further outside from the sun. The spectra became steeper within low speed plasma and flatter in high-speed plasma but were flatter overall than outside 0.40 AU. There was no evident dependence on heliographic latitude varying over more than 12° because given parts of a stream occurred at completely different latitudes.

Altogether, if the observed change in the spectral characteristics of magnetic field fluctuations would not be an effect of heliographic distance (besides the dependence on the solar wind stream structure), the flatter spectra at perihelion must have been caused by a time variation just during the time, when the two HELIOS spacecraft were inside 0.40 AU

covering a heliographic longitude range of 200°. Outside 0.40 AU, no comparable flattening of the spectra was observed in this longitudinal range by HELIOS 1 and 2 during three solar rotations each. Therefore, we conclude that the reason for the observed change in the spectra of magnetic field fluctuations mainly is the increasing distance from the sun. Besides this, the spectra are different at different locations in a high speed solar wind stream.

In the frequency range under consideration there are earlier studies of the radial variation of power spectra of the interplanetary magnetic field. *Blake and Belcher* [1974] calculated power spectra of the interplanetary field measured by Mariners 4 and 5 between 0.7 and 1.6 AU. They found that 'except for a general decrease in the overall power level .... the spectra show no striking dependence on radius in the range between 0.7 and 1.6 AU.' This is in agreement with our findings, e.g., the best fit exponents do not vary significantly in a distance range from 0.7 to 1.0 AU. But inside 0.40 AU (maybe a little further out) we found physical processes effective in changing the spectral behavior of magnetic field fluctuations. We cannot offer a straight-forward explanation for the spectra being quite different inside and outside approximately 0.40 AU (the distance of 0.40 AU is not a sharp boundary and may well be 0.50 AU or 0.35 AU under different solar wind conditions). With HELIOS 2 plasma and magnetic field data *Denskat et al.* [1978] showed for the same time interval considered here the fluctuations to be predominantly of Alfvénic nature (76% of the time), were more than 90% of the Alfvénic fluctuations were propagating outward.

For an explanation of the observed frequency spectra of Alfvénic turbulence in the solar wind with their associated changes as a function of distance, one could in principle invoke nonlinear coupling between different frequencies or frequency dependent damping or excitation or propagation effects. If we follow *Dobrowolny et al.* [1980b], nonlinear interactions would require a mixture of outward and inward propagating Alfvénic disturbances. *Denskat et al.* [1978], using both magnetic field and plasma data only found outwardly propagating Alfvénic fluctuations during the time periods analyzed but did not explicitly separate low-frequency fluctuations. Following this line of reasoning, nonlinear cascading could only explain the observed radial evolution of turbulence spectra if nonlinear effects are due to the non-Alfvénic 'impurities' (e.g., showing up in the magnitude spectra and not included in Dobrowolny's treatment). We note finally that formally the spectral index α = 3/2 for incompressible MHD turbulence [*Kraichnan*, 1965] and outward propagating Alfvénic turbulence [*Dobrowolny et al.*, 1980a, b] agrees with observations only at the higher frequency end.

Additional possibilities to explain the observations are a damping of Alfvénic fluctuations that increases with frequency or a generation effect that decreases with frequency. A difficulty here is the theoretical result [*Barnes*, 1966] that linear Alfvén waves at least propagate without damping in a collisionless medium. For nonlinear Alfvénic waves a theory of damping and excitation is restricted to only a few isolated papers [*Lee and Völk*, 1973; *Cohen and Dewar*, 1974].

If one tries to explain the filtering of the fluctuations by using models of Alfvén wave propagation in the solar wind, one is faced with existing theories for plane nonlinear Alfvén waves [*Barnes and Suffolk*, 1971; *Barnes and Hollweg*, 1974;

Hollweg, 1974; *Barnes*, 1976], which actually cannot be applied to the Alfvénic fluctuations observed in the solar wind plasma [*Burlaga*, 1979]. The latter will be shown in the next chapter for the fluctuations observed by the HELIOS spacecraft. *Whang* [1973] and *Goldstein et al.* [1974] have shown that there exist large amplitude fluctuations that satisfy a linear Alfvén wave equation and need not be plane waves. The observed fluctuations may represent these general large-amplitude Alfvén waves, for which a propagation theory is totally missing. On the other hand, plane wave theories cannot be applied either, since the observed fluctuations are nonplanar.

5. INFORMATION ON THE TYPE OF FLUCTUATION AT DIFFERENT HELIOGRAPHIC DISTANCES

A technique very often used in studying MHD fluctuations in the solar wind is the minimum variance method [*Sonnerup and Cahill*, 1967]. Although there is evidence that the direction of minimum variance is not indicative of the wave normal direction for Alfvénic fluctuations [*Solodyna and Belcher*, 1976; *Denskat and Burlaga*, 1977], we use the minimum variance method at different heliographic distances for comparison of the geometric orientation of the covariance matrix. The distributions of the ratios of eigenvalues of the magnetic field variance ellipsoids for one hour intervals are very similar to those previously published [e.g., *Denskat and Burlaga*, 1977] and need not be shown. Although there might be some differences in the distributions of the ratios of eigenvalues at different heliographic distances, the effect is very small if actually existing.

Figure 6 shows that the distributions for the angle between the minimum variance normal and the mean field direction are different for perihelion and aphelion solar wind magnetic field conditions, where the results for the aphelion period is consistent with previous findings [e.g., *Burlaga and Turner*, 1976]. Owing to the large number of cases involved in this method, we consider this difference to be statistically significant. In addition, HELIOS 1 and HELIOS 2 reveal basically the same results.

Several reasons may be responsible for the differences at perihelion and aphelion. The main reason is very likely the different contribution of higher frequency waves at perihelion and aphelion to the overall power in the one hour time periods analyzed. Under aphelion conditions the low-fre-
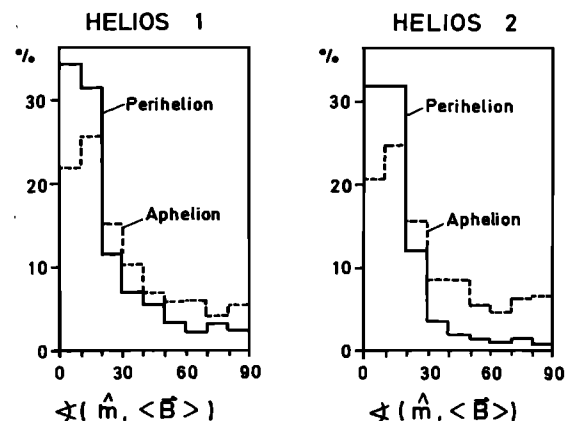
Fig. 6. Distribution of the angles between the average magnetic field and the minimum variance direction. The aphelion and perihelion distance intervals are the same as in Figure 1.

quency fluctuations are quite predominant in power. This predominance is essentially reduced under perihelion conditions where a larger contribution of higher frequency fluctuations with different propagation vectors forces the minimum variance direction to be more aligned with the mean field direction. This interpretation is also valid for a MHD turbulence containing a wide spectrum of propagation directions. Another possibility to explain the minimum variance results is a possible difference in the contribution of tangential discontinuities to the power at perihelion and aphelion. This must yet be studied in detail and is beyond the scope of this paper. A third reason may be the difference in average field orientation, i.e., more radial at perihelion. Since simple pictures of symmetric radial solar wind flow lead to wave vectors radially directed from the sun [Völk and Alpers, 1973], one would expect in this picture large differences for minimum variance results at perihelion and aphelion. The differences are not so great, and the picture of symmetric radial flow is too simple as well. The change in the distributions of minimum variance normals, however, points in the expected direction, i.e. the distributions are broader at aphelion.

The unambiguous identification of MHD wave modes is generally insufficient from magnetic field data from one spacecraft. However, there exist specific phase relationships between magnetic field components and between magnetic field components and magnitude by means of which some specific mode properties can be proven. These relationships can be determined by cross spectral analysis methods. Using interplanetary magnetic field conditions when the field was directed along the heliocentric radius, Sari [1977] applied this technique and found the field fluctuations being dominated by the general finite amplitude Alfvén wave.

We used these phase relationships to study the fluctuations in HELIOS 2 data from 1.0 AU to 0.29 AU. Since we did not limit our study to specific conditions of the dc-magnetic field, we cannot exclude, e.g., TD's from our analysis. We found over the whole heliographic distance range analyzed a large amplitude nonplanar wave mode being present most of the time, most clearly in central parts and trailing edges of high speed streams. In this wave mode the magnetic field perturbation vector moves on a sphere |B| = constant. With the exception of the perturbation vector moving on a circle of this sphere (called a transverse wave) this implies the magnetic field fluctuations perpendicular and parallel to the average field direction must be correlated. Two examples in Figure 7 show the relevant coherencies between magnetic field fluctuations perpendicular and parallel to the average field direction for aphelion and perihelion conditions. These results are quite typical. The coherencies in trailing edges of high speed streams generally ranged from 0.6 to 0.95 and the phase was quite stable around 180°. No significant differences between coherencies and phases at different heliographic distances were found. There are cases when the coherence for almost all frequencies is between 0.85 and 0.95. However, the coherence is never greater, indicating other types of fluctuations being present during each 11 1/2 hour of the analysis. But this is expected since at least TD's are present all of the time. Barnstorf [1980] has demonstrated the occurence of TD's at all heliographic distances covered by the HELIOS spacecraft.

In leading edges of high speed streams we found evidence for magnetosonic waves and/or convected stationary struc-

HELIOS 2

JANUARY 24,1976, 0.97 AU

APRIL 14,1976, 0.29 AU
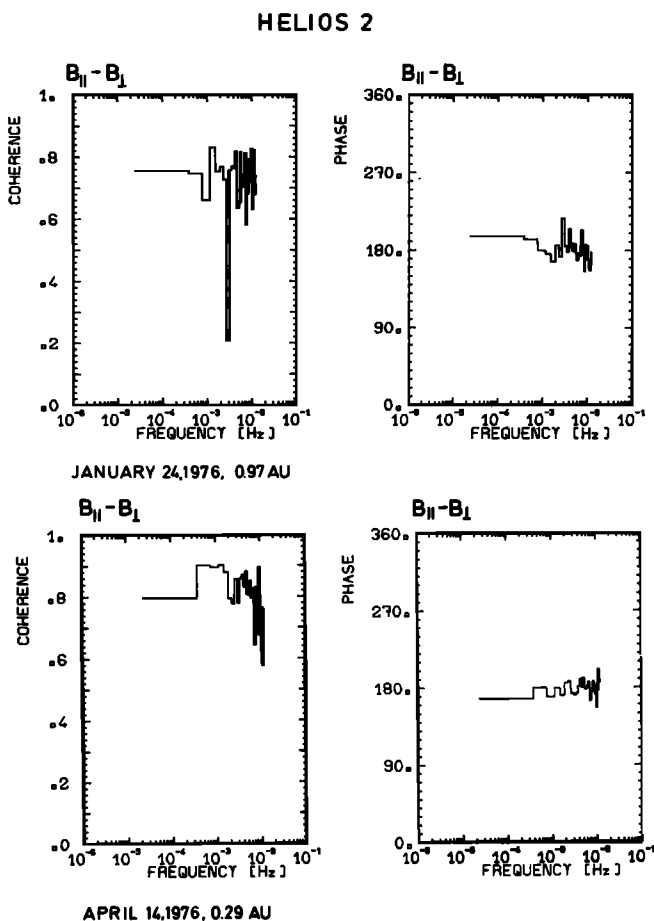
Fig. 7. Two representative examples of coherencies and phases between magnetic field fluctuations perpendicular $B_\perp$ and parallel to the average field direction $B_\parallel$ at 0.97 AU and 0.29 AU. The confidence intervals for the coherence and phase depend on the size of the coherence [Jenkins and Watts [1968], p. 379ff]. For example, the 95% confidence limits of a coherence of 0.85 range from 0.70 to 0.92 for the coherence and are ±9.5° for the phase. All phases shown are consistent with 180° within the confidence limits.

tures (coherencies between magnetic field components and magnitude up to 0.9 and phases at 0°). No evidence for such modes was found in central parts and trailing edges of high speed streams and in low speed plasma (relevant coherencies < 0.4).

The transverse wave mode mentioned above must have the squares of the two components perpendicular to the average field direction correlated. We only found one 11 1/2-hour time interval out of 161 analysed from HELIOS 2, where B_X^2 and B_Y^2 were significantly correlated with coherencies up to 0.65 and phases at 180°. During all other time intervals analysed the coherencies were less than 0.4.

For future theoretical treatments of this general large amplitude nonplanar wave mode the spatial evolution of the ratio of the power parallel to the power perpendicular to the average direction of the magnetic field inherent in this sort of fluctuations may be of interest. Therefore we computed the ratio $P_\parallel/P_\perp$ ($P_\parallel$ and $P_\perp$ are the power densities parallel and perpendicular to the average field direction, respectively) from the HELIOS 2 data for 11 1/2-hour time intervals over the distance range from 0.29 to 1.0 AU. The most striking property of this ratio $P_\parallel/P_\perp$ is its high variability as a function of radius with values between 0.08 and 0.8, the latter being quite rare, however. Apparently there exists a quite stronger

dependence of this ratio on the solar wind stream structure than on the heliographic distance. The ratio $P_\parallel/P_\perp$ is only greater than 0.4 outside trailing edges of high speed streams with typical values between 0.15 to 0.3 within trailing edges. However, the ratio $P_\parallel/P_\perp$ is not the same for all frequencies, but is the smallest for the lowest frequency analysed and increases slightly with increasing frequency.

6. SUMMARY AND CONCLUSIONS

HELIOS observations at heliographic distances between 0.29 and 1.0 AU show that nonfrequency dependent statistical properties of directional MHD fluctuations in the solar wind do not change significantly with increasing radius, with the exception of the distribution of minimum variance normals that are broader at aphelion than at perihelion. For the latter, several explanations are possible; the main reason for the difference in the distributions is very likely the different power density contribution of high-frequency waves at different heliographic distances.

From power spectral analysis of the vector components and the field magnitude (frequencies between 2.4×10^{-5} Hz to 1.3×10^{-2} Hz) we conclude that the fluctuations as a function of frequency evolve differently up to about 0.4 AU and further outside. The MHD spectra from 0.29 to 0.40 AU are generally flatter than the ones further outside with the greatest differences at low frequencies. The solar wind seems to act as a low-pass filter for MHD fluctuations. Assuming a power law dependence of the spectra with $P \sim f^{-\alpha}$ the spectral exponent α inside 0.40 AU is close to 1 for the components and field magnitude. However, at this distance from the sun a power law fit over frequencies from 2.4×10^{-5} Hz to 1.3×10^{-2} Hz is not completely satisfactory, since the spectral densities are the flattest at low frequencies and are becoming steeper with increasing frequency. Outside 0.40 AU the spectral exponent lies between 1.5 and 1.6. At all distances there is a high variability of spectral exponents. The variation with distance of the spectra is most pronounced in central parts and trailing edges of high speed streams. Concerning the spectral densities of different frequency bands as a function of radius, we found a different behavior of vector components and field magnitude, especially if spectral densities normalized by the squares of average field magnitudes were computed. While normalized field magnitude spectral densities of all frequencies remained relatively constant over all heliographic distances, the normalized vector component spectral densities remained almost of the same size over all distances only for the low-frequency fluctuations (frequencies $<1.6 \cdot 10^{-3}$ Hz) but decreased to 1/4 from 0.29 to 1.0 AU for all higher frequency fluctuations (frequencies $>1.6 \cdot 10^{-3}$ Hz). An interpretation of the observed spectral properties does not seem possible with existing theories.

As shown in the last chapter, most of the fluctuations are in the general large amplitude nonplanar wave mode, at least in central parts and trailing edges of high-speed streams. This general nonplanar wave mode exists at all frequencies investigated. This fact must be kept in mind if one tries to explain the spectra becoming steeper with increasing radius. The ratio of power parallel to power perpendicular to the average magnetic field direction is quite variable and depends more on the streaming structure of the solar wind than on heliographic distance. Evidence for magnetosonic waves

and/or convected structures was found in leading edges of high-speed streams.

REFERENCES

Barnes, A., Collisionless damping of hydromagnetic waves, *Phys. Fluids, 9,* 1483, 1966.

Barnes, A., On the nonexistence of plane-polarized large amplitude Alfvén waves, *J. Geophys. Res., 81,* 281, 1976.

Barnes, A., Hydromagnetic waves and turbulence in the solar wind, in *Solar and Solar Wind Plasma Physics,* vol. 1., edited by E. N. Parker, C. F. Kennel, and L. J. Lanzerotti, North-Holland, Amsterdam, 1979.

Barnes, A., and J. V. Hollweg, Large-amplitude hydromagnetic waves, *J. Geophys. Res., 79,* 2302, 1974.

Barnes, A., and G. C. J. Suffolk, Relativistic kinetic theory of the large-amplitude transverse Alfvén wave, *J. Plasma Phys., 5,* 315, 1971.

Barnstorf, H., Stromschichten im interplanetaren Plasma, Ph.d. dissertation, Technische Universität Braunschweig, Braunschweig, Federal Republic of Germany, 1980.

Belcher, J. W., and R. Burchsted, Energy densities of the Alfvén waves in the interplanetary medium, 2, *J. Geophys. Res., 79,* 4765, 1974.

Belcher, J. W., and L. Davis, Jr., Large-amplitude Alfvén waves in the interplanetary medium, 2, *J. Geophys. Res., 76,* 3534, 1971.

Belcher, J. W., L. Davis, Jr., and E. J. Smith, Large-amplitude Alfvén waves in the interplanetary medium: Mariner 5, *J. Geophys. Res., 74,* 2302, 1969.

Bendat, J. S., and A. G. Piersol, Random data: Analysis and measurement procedures, Interscience, New York, 1971.

Blake, D. H., and J. W. Belcher, Power spectra of the interplanetary magnetic field, 0.7–1.6 AU, *J. Geophys. Res., 79,* 2891, 1974.

Burlaga, L. F., Hydromagnetic waves and discontinuities in the solar wind, *Space Sci. Rev., 12,* 600, 1971.

Burlaga, L. F., Magnetic fields, plasmas, and coronal holes: The inner solar system, *Space Sci. Rev., 23,* 201, 1979.

Burlaga, L. F., and J. B. Turner, Microscale 'Alfvén waves' in the solar wind at 1 AU, *J. Geophys. Res., 81,* 73, 1976.

Cohen, R. H., and R. L. Dewar, On the backscatter instability of solar wind Alfvén waves, *J. Geophys. Res., 79,* 4174, 1974.

Coleman, P. J., Jr., Hydromagnetic waves in the interplanetary plasma, *Phys. Rev. Lett., 17,* 207, 1966.

Coleman, P. J., Jr., Turbulence, viscosity, and dissipation in the solar wind plasma, *Astrophys. J., 153,* 371, 1968.

Coleman, P. J., Jr., E. J. Smith, L. Davis, Jr., and D. E. Jones, The radial dependence of the interplanetary magnetic field: 1.0–1.5 AU, *J. Geophys. Res., 74,* 2826, 1969.

Denskat, K. U., and L. F. Burlaga, Multispacecraft observations of microscale fluctuations in the solar wind, *J. Geophys. Res., 82,* 2693, 1977.

Denskat, K. U., F. M. Neubauer, and R. Schwenn, Properties of 'Alfvénic' fluctuations near the sun: HELIOS 1 and HELIOS 2, paper presented at the Fourth Solar Wind Conference, Burghausen, Federal Republic of Germany, August 28–September 1, 1978.

Dobrowolny, M., A. Mangeney, and P. Veltri, Properties of magnetohydrodynamic turbulence in the solar wind, *Astron. Astrophys., 83,* 26, 1980a.

Dobrowolny, M., A. Mangeney, and P. Veltri, Fully developed asymmetric hydromagnetic turbulence in the interplanetary space, *Phys. Rev. Lett., 45,* 144, 1980b.

Goldstein, M. L., A. J. Klimas, and F. D. Barish, On the theory of large-amplitude Alfvén waves, in *Solar Wind Three,* edited by C. T. Russell, p. 385, University of California Press, Los Angeles, 1974.

Hedgecock, P. C., A correlation technique for magnetometer zero level determination, *Space Sci. Instrum., 1,* 83, 1975a.

Hedgecock, P. C., Measurements of the interplanetary magnetic field in relation to the modulation of cosmic rays, *Solar Phys., 42,* 497, 1975b.

Hollweg, J. V., Transverse Alfvén waves in the solar wind: Arbitrary k, V_0, B_0, and $|\delta B|$, J. Geophys. Res., 79, 1539, 1974.

Jenkins, G. M., and D. G. Watts, Spectral analysis and its application, Holden-Day, San Francisco, Calif. 1968.

Kraichnan, R. H., Inertial-range spectrum of hydromagnetic turbulence, Phys. Fluids, 8, 1385, 1965.

Lee, M. A., and H. J. Völk, Damping and nonlinear wave-particle interactions of Alfvén-waves in the solar wind, Astrophys. Space Sci., 24, 31, 1973.

Marsch, E., K. H. Mühlhäuser, R. Schwenn, H. Rosenbauer, W. Pilipp, and F. M. Neubauer, Solar wind protons: Three-dimensional velocity distributions and derived plasma parameters measured between 0.3 and 1 AU, J. Geophys. Res., 87, 52, 1982.

Musmann, G., F. M. Neubauer, A. Maier, and E. Lammers, Das Förstersonden-Magnetfeldexperiment (E2), Raumfahrtforschung, 19, 232, 1975.

Musmann, G., F. M. Neubauer, and E. Lammers, Radial variation of the interplanetary magnetic field between 0.3 AU and 1.0 AU; Observations by the HELIOS 1 spacecraft, J. Geophys., 42, 591, 1977.

Owens, A. J., An algorithm for generating fluctuations having an arbitrary power spectrum, J. Geophys. Res., 83, 1673, 1978.

Rosenbauer, H., R. Schwenn, E. Marsch, B. Meyer, H. Miggenrieder, M. D. Montgomery, K. H. Mühlhäuser, W. Pilipp, W.

Voges, and S. M. Zink, A survey on initial results of the Helios plasma experiment, J. Geophys., 42, 561, 1977.

Rosenberg, R. L., M. G. Kivelson, P. J. Coleman, Jr., and E. J. Smith, The radial dependences of the interplanetary magnetic field between 1 and 5 AU: Pioneer 10, J. Geophys. Res., 83, 4165, 1978.

Sari, J. W., On the existence of finite amplitude, transverse Alfvén waves in the interplanetary magnetic field, Rep. X-692-77-170, Goddard Space Flight Center, Greenbelt, Md., 1977.

Solodyna, C. V., and J. W. Belcher, On the minimum variance direction of magnetic field fluctuations in the azimuthal velocity structure of the solar wind, Geophys. Res. Lett., 3, 565, 1976.

Sonnerup, B. U. Ö., and L. H. Cahill, Jr., Magnetopause structure and attitude from Explorer 12 observations, J. Geophys. Res., 72, 171, 1967.

Völk, H. J., and W. Alpers, The propagation of Alfvén waves and their directional anisotropy in the solar wind, Astrophys. Space Sci., 20, 267, 1973.

Whang, Y. C., Alfvén waves in spiral interplanetary field, J. Geophys. Res., 78, 7221, 1973.